Journal of Catalysis **206,** 71–81 (2002)
doi:10.1006/jcat.2001.3476, available online at http://www.idealibrary.com on IDEAL®

# Cu–MgO Samples Prepared by Mechanochemistry for Catalytic Application

M. Varga,* Á. Molnár,*,[1] G. Mulas,† M. Mohai,‡ I. Bertóti,‡ and G. Cocco†

*Department of Organic Chemistry, University of Szeged, Dóm tér 8, Szeged H-6720, Hungary; †Dipartimento di Chimica, Universitá di Sassari, Via Vienna 2, I-07100 Sassari, Italy; and ‡Research Laboratory of Materials and Environmental Chemistry, Chemical Research Center, Hungarian Academy of Sciences, P.O. Box 17, Budapest H-1525, Hungary

Received June 26, 2001; revised October 30, 2001; accepted November 30, 2001; published online January 14, 2002

**High-energy ball milling was applied to prepare powder samples by treating copper or copper oxides with magnesium or magnesium oxide. The five samples thus prepared were characterized by physical methods. According to X-ray diffraction the mechanical treatment resulted in the formation of nanostructured powders. Carbon and oxygen impurities and Mg (mainly as oxide) were detected by X-ray photoelectron spectroscopy of the as-milled samples. Four samples, namely, nanocomposite materials prepared by the self-sustaining reaction of copper oxides and magnesium applied in stoichiometric amounts [$(Cu_2O)Mg$ and $(CuO)Mg$] and samples produced by mechanical treatment of copper oxides and magnesium oxide [$(Cu_2O)_7(MgO)_{93}$ and $(CuO)_{13}(MgO)_{87}$] also had copper on the surface. The latter specimens and 3% Cu + MgO were unique in their characteristics to have, after a short hydrogen treatment or after catalytic application, an unusually large concentration of $Cu^0$ measured by the $N_2O$ titration method. Temperature-programmed reduction showed, in each case, the existence of reducible copper species on the surface. The quantity of reducible copper was quite low for $(Cu_2O)Mg$, $(CuO)Mg$, and 3% Cu + MgO, whereas almost the total amount of copper of $(Cu_2O)_7(MgO)_{93}$ and $(CuO)_{13}(MgO)_{87}$ was available for reduction. Two types of copper species have been detected: bulk CuO with a reduction temperature of about 260°C [characteristic of $(CuO)Mg$ and also found in $(Cu_2O)Mg$] and species strongly interacting with the support with a reduction temperature of about 350°C [3% Cu + MgO, $(Cu_2O)_7(MgO)_{93}$, $(CuO)_{13}(MgO)_{87}$, and also detected in $(Cu_2O)Mg$]. The 3% Cu + MgO, exhibited the highest basicity measured by the decomposition of 2-methyl-3-butyn-2-ol and the dimerization of acetone. The samples showed high activity in the dehydrogenation of 2-propanol, whereas their activity in the one-step synthesis of methyl isobutyl ketone from acetone was moderate. Methyl isobutyl ketone (MIBK) was formed in low selectivity over the samples prepared by a self-sustaining reaction and 3% Cu + MgO, whereas very high MIBK selectivities were observed over the mixed oxides. These features were correlated with the relative concentration of active sites capable of hydrogenating the carbon–oxygen and carbon–carbon double bond.** 

[1] To whom correspondence should be addressed. Fax: (36) 62-544-200. E-mail: amolnar@chem.u-szeged.hu.

*Key Words:* **copper; magnesium oxide; mechanochemistry; methyl isobutyl ketone; basicity; $Cu^0$ specific surface.**

## INTRODUCTION

Mechanical treatment by high-energy ball milling is recognized as a powerful method to obtain a variety of highly dispersed systems and nonequilibrium phases in powder form via solid-state reactions. Mechanical alloying of pure elements and mechanical milling of equilibrium intermetallics are used to prepare a variety of amorphous alloys and nanocrystalline materials (1, 2). Moreover, mechanically induced self-sustaining reactions, occurring in highly exothermic systems, allow the production of dispersed metal–metal oxide systems via an oxygen displacement reaction (3, 4). Recently, attention has been paid to the potentialities of materials prepared by such techniques as heterogeneous catalysts (5–8).

We have also been involved in recent years in exploring the possibilities to apply such systems as catalytic materials. We have shown that copper-on-magnesia catalysts prepared by such unconventional methods exhibit promising characteristics in the one-step conversion of acetone to MIBK in the presence of hydrogen (9, 10). MIBK is an important chemical used as solvent and is applied in the production of paints and stabilizers (11). At present it is prepared in industry by the three-step process. Results published in the last decade, however, showed that the one-step synthesis offers a simpler technology. This procedure requires bifunctional catalysis: an acidic or basic support material acts to induce the formation of diacetone alcohol through aldol dimerization which then undergoes dehydration under reaction conditions (at 250–300°C) to form mesityl oxide (MO). The final step is the hydrogenation of the carbon–carbon double bond catalyzed by a metal. The best combinations include Ni (12), Pt (13) or Pd (14–18), and MgO (14), acidic solids such as HZSM5 (13) or niobic acid (15, 16), and hydrotalcite-like materials (12, 17, 18).



0021-9517/02 $35.00

**TABLE 1**

**Samples Prepared and Studied**

| Composition of synthesis mixture | Milling time (h) | Sample denomination | Composition (wt%) Cu | Composition (wt%) MgO |
|---|---|---|---|---|
| $Cu_2O + Mg$[a] | 1[b] | $(Cu_2O)Mg(1)$ | 75.9 | 24.1[c] |
| Same | 13[b] | $(Cu_2O)Mg(13)$ | Same | Same |
| Same | 30[b] | $(Cu_2O)Mg(30)$ | Same | Same |
| $CuO + Mg$[a] | 30[b] | (CuO)Mg | 61.2 | 38.8[c] |
| 3 at% Cu + 97 at% MgO | 32 | 3% Cu + MgO | 4.6 | 95.4 |
| 7 at% $Cu_2O$ + 93 at% MgO | 51 | $(Cu_2O)_7(MgO)_{93}$ | 18.7 | 78.9 |
| 13 at% CuO + 87 at% MgO | 54 | $(CuO)_{13}(MgO)_{87}$ | 18.2 | 77.2 |

[a] In stoichiometric amount.
[b] After the completion of the self-sustaining reaction.
[c] Assuming complete oxidation of Mg during self-sustaining reaction.

In our first studies we applied amorphous bicomponent Cu–Mg alloys fabricated by rapid quenching or mechanical alloying and used as catalyst precursors (9, 10). Most of these samples exhibited excellent activity in the dehydrogenation of 2-propanol attributed to the high proportion of copper relative to magnesium in the precursor materials. In the transformation of acetone to MIBK, however, their overall performance was inferior to the catalysts prepared by impregnation or coprecipitation (19). It was an obvious conclusion, therefore, that the preparation of new samples with decreased copper content is required. Having an appropriate balance of the metallic (copper) and basic (MgO) active sites the new samples are expected to exhibit improved catalytic performance. In addition, we also intended to explore the mechanochemical synthesis and catalytic application of all other candidates of the Cu(O)–Mg(O) system. As a logical step to the completion of our study in this field, in this paper we disclose the preparation and characterization of five new Cu-on-MgO samples prepared by mechanochemistry and their application in the synthesis of MIBK.

## EXPERIMENTAL

### *Materials*

2-Propanol, acetone (Reanal products), and 2-methyl-3-butyn-2-ol (Fluka) were of at least 99% purity. Cu powder (99.5%), $Cu_2O$ (97%), CuO (98%), and MgO (99%) were purchased from Aldrich, whereas Mg powder (99.8%) was an Alfa product. Linde high-purity hydrogen (99.98%), helium (99.999%), and 11% hydrogen in argon were used.

### *Preparation of Samples*

Mechanical treatments were performed using a Spex Mixer/Mill (Mod. 8000) working at 875 rpm and equipped with hardened stainless-steel vials and balls. Changes in the vial temperature during self-sustaining reactions were monitored by a thin lamella-shaped Pt resistance thermometer fixed on the outside wall of the milling vial. The powder handling and sampling were performed under purified argon atmosphere in an MBraun M150 glove box ($O_2$ and $H_2O$ at ppm level). Information about the composition of the synthesis mixture and the as-milled samples, milling time, and sample denomination is collected in Table 1.

### *Sample Characterization Techniques*

X-ray diffraction (XRD) analysis was carried out by a Siemens D500 diffractometer using Cu$K\alpha$ radiation. To estimate the coherent diffraction domain sizes and microstrain of the observed crystal phases, a full profile refinement analysis of the patterns was performed following the Rietveld method (20, 21). Differential scanning calorimetry (DSC) was performed with a power compensation Perkin–Elmer DSC-7 (scanning rate = 20 degrees $min^{-1}$).

X-ray photoelectron spectra were recorded on a Kratos XSAM 800 spectrometer operated at a fixed analyzer transmission mode using Mg$K\alpha_{1,2}$ (1253.6 eV) excitation. The pressure of the analysis chamber was lower than $10^{-7}$ Pa. Photoelectron lines of the main constituent elements, Cu2p, O1s, C1s, and Mg2p, were recorded by 0.1-eV steps. Spectra were referenced to the C1s line of the hydrocarbon-type carbon set at 284.6 eV. Spectra were processed by the Vision 2000 and X-ray photoelectron spectroscopy (XPS) MultiQuant programs (22, 23) using the experimentally determined photoionization cross-section data of Evans *et al.* (24) and the asymmetry parameters of Reilman *et al.* (25).

Temperature-programmed reduction (TPR) was carried out in the temperature range between room temperature and 570°C with a gas mixture containing 11% hydrogen in argon (flow rate = 10 ml $min^{-1}$, sample size = 20 mg, temperature ramp = 10 degrees $min^{-1}$). Measurements were made on samples as received or after oxidative pretreatment in air (30 min at 200°C, flow rate = 10 ml $min^{-1}$).

The $Cu^0$ surface area of the samples was measured by $N_2O$ titration based on the reaction of nitrous oxide with $Cu^0$ species using the GC pulse method. A short hydrogen treatment (30 min, 290°C, 20 ml $min^{-1}$) was applied before measurements.

Decomposition of 2-methyl-3-butyn-2-ol in pulse microreactor experiments was used to characterize the basicity of samples (26). After the appropriate pretreatment (300°C, 1 h, 30 ml hydrogen $min^{-1}$, then 30 min in 30 ml helium $min^{-1}$), the samples were treated with pulses of the reactant at 200°C in helium (20 ml $min^{-1}$). A 15% PEG 20M on a Chromosorb W column was used for GC analysis. Under these conditions the products of cleavage (acetone and acetylene) were formed in approximately equal amounts. Information about the ability of the samples to induce dimerization of acetone was acquired by reacting acetone in helium in a flow system (100 mg of catalyst, pretreatment at 300°C, 1 h, measurement at 300°C, 10 ml helium $min^{-1}$, 0.02 ml acetone $h^{-1}$). The concentration of mesityl oxide, the product of condensation (dimerization followed by dehydration), was measured.

*Catalytic Measurements*

Catalytic tests were carried out in a flow-type Pyrex glass microreactor (8 mm i.d., vertical position, fritted glass catalyst holder) with a catalyst quantity of about 150 mg. Catalyst samples were treated in flowing hydrogen (300°C, 1 h, 30 ml $min^{-1}$) before measurements. The liquid reactant was fed by a motorized syringe pump into a stainless-steel evaporator kept at 80°C, mixed with an appropriate amount of hydrogen or hydrogen + helium mixture controlled by a mass flow controller (Aalborg, GFM17), and then introduced into the reactor which was kept at reaction temperature. The reactor temperature was controlled to an accuracy of 0.5°C by using a microprocessor-based controller (Self-tune plus, LOVE Controls Corp.). The effluents, sampled by a pneumatic gas sampling system, were analyzed by GC (Shimadzu 8A equipment, thermal conductivity detector, CWAX 20M column, 100°C, 30 ml $min^{-1}$ flow rate of helium carrier gas). A Data Apex Chromatography Station for Windows 1.5 was applied for chromatographic data acquisition and processing.

## RESULTS AND DISCUSSION

*Characterization of the As-Milled Samples*

Cu–MgO nanocomposite materials were prepared by the self-sustaining reaction (SSR) induced by the mechanical treatment of copper(I) oxide and magnesium [$(Cu_2O)Mg$] or copper(II) oxide and magnesium [(CuO)Mg] applied in stoichiometric amounts ($Cu_2O$ to Mg and CuO to Mg ratios are 1). The occurrence of self-sustaining reactions under milling is characterized by a sudden conversion into products, which occurs after an induction period, the ignition

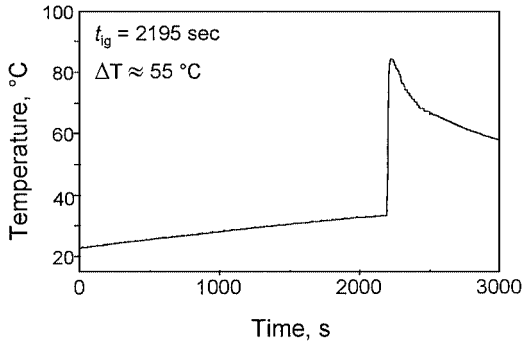


**FIG. 1.** Change in the vial temperature as a function of milling time during the synthesis of (CuO)Mg [self-sustaining high-temperature synthesis induced by mechanical treatment of the stoichiometric mixture (1 : 1 molar ratio) of CuO and Mg].

time ($t_{ig}$). The chemical transformation, that is, the oxygen displacement leading to the formation of Cu and MgO can be detected by a steep rise in the temperature of the milling vial ($\Delta T$). In Fig. 1, the temperature trace of the external side of the vial monitored during the milling of a stoichiometric mixture of CuO and Mg is plotted as a function of the milling time. XRD of the material thus formed shows that the process leads to the formation of crystalline Cu and MgO (Fig. 2, pattern a; note the intense double peak at $2\theta$ 42.9 and 43.3 corresponding to the 200 reflection of MgO and the 111 reflection of Cu, respectively). To increase the Cu dispersion in the MgO matrix, the combusted powders were then subjected to further milling (30 h). As a result, a high strain content and nanostructured dimension were obtained, as suggested by the peak-broadening phenomena (Fig. 2, pattern b, see the coalescence of the main peaks

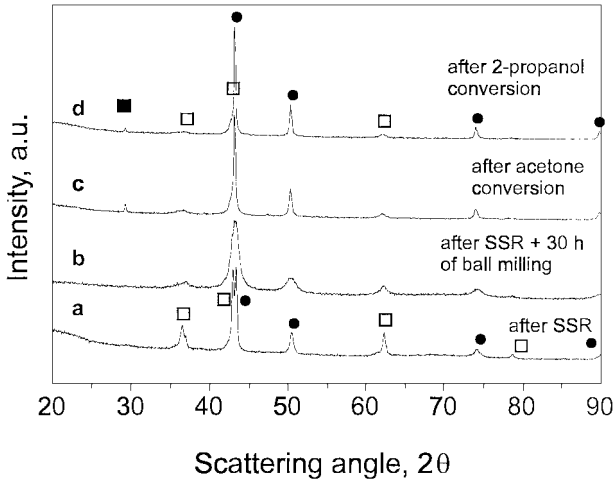


**FIG. 2.** XRD patterns of (CuO)Mg. (a) After self-sustaining reaction, (b) self-sustaining reaction followed by further ball milling for 30 h, (c) after reaction of acetone (6 h), (d) after reaction of 2-propanol (15 h). ●, Cu (4–836); □, MgO (4–829); ■, MgO (30–794). The numbers of the corresponding JCPDS card files are given in parentheses.

**TABLE 2**

**Particle-Size Data Estimated from XRD and Specific Copper Surface Area Determined by $N_2O$ Decomposition**

| Sample | Particle size (nm) | | $Cu^0$ ($m^2\ g^{-1}$) |
|---|---|---|---|
| | Cu | MgO | |
| $(Cu_2O)Mg(1)$ | 45 | 60 | 0 |
| $(Cu_2O)Mg(13)$ | 10 | 14 | 1.10 |
| $(Cu_2O)Mg(30)$ | 9.4 | 8.0 | 1.30 |
| After reaction (acetone)[a] | n.d.[f] | n.d.[f] | 1.45 |
| (CuO)Mg (after SSR) | 24 | 43 | n.d. |
| (CuO)Mg (after SSR + 30 h milling) | 5.5 | 6.1 | 10.55 |
| After reaction (2-propanol)[b] | 24 | 12–15 | n.d. |
| After reaction (acetone)[a] | 35 | 8.4 | 8.2 |
| 3% Cu + MgO | 6.1 | 10 | 1.50 |
| After reaction (acetone)[c] | 22 | 13 | 1.50 |
| $(Cu_2O)_7(MgO)_{93}$ | (2.6)[d] | 10 | 13.8 |
| After reaction (acetone)[e] | n.d.[f] | n.d. | 12.5 (7.90)[g] |
| $(CuO)_{13}(MgO)_{87}$ | (1.5)[h] | 9 | 16.3 |
| After reaction (acetone)[e] | 41 (8)[h] | 10 | 11.6 (7.10)[g] |

[a] 280°C, 6 h.
[b] 300°C, 12 h.
[c] 300°C, 6 h.
[d] Particle size of $Cu_2O$.
[e] 280°C, 1 h.
[f] Not determined.
[g] 280°C, 24 h.
[h] Particle size of CuO.

of Cu and MgO) and estimated by full profile refinement analysis of the same pattern according to Rietveld (20, 21). Particle-size data estimated by this method for all samples including data determined after reactions are collected in Table 2.

During the chemical tests, a small increase in the dimension of both Cu and MgO crystallites occurred in the (CuO)Mg sample (Table 2; see also the decrease in the line broadening in patterns c and d of Fig. 2). Moreover, the small signal at $2\theta = 29.25$ suggests the formation of a small amount of another MgO phase with cubic symmetry (JCPDS 30-794), even if the attribution based on a single peak can be questioned.

The behavior of the $Cu_2O + Mg$ mixture during the mechanical treatment was similar to that of the (CuO)Mg sample. The self-sustaining reaction occurred after 3140 s of milling time, and a $\Delta T$ of 32.9°C was measured (27). The temperature jump value, naturally, depends on the heat capacity of the whole milling system. However, since both self-sustaining reactions were performed in the same apparatus, the two values measured in the $CuO + Mg$ and $Cu_2O + Mg$ reactions ($\Delta T = 55$ and 32.9°C, respectively) reflect the different enthalpy change occurring in the two self-sustaining processes. Moreover, some unreacted $Cu_2O$ was still present which, however, disappeared during the further milling treatment, and nanosize Cu–MgO powders were obtained.

The 3% Cu + MgO sample was obtained by milling pure Cu and MgO (Fig. 3, pattern a). Nanostructured domains of Cu and MgO were obtained as a result of the mechanical treatment, and their dimensions changed somewhat during acetone conversion (Fig. 3, pattern b and Table 2). As reported earlier, the new MgO phase (JCPDS 30-794) can also be detected in the XRD pattern.

Two mixed oxides, $(Cu_2O)_7(MgO)_{93}$ and $(CuO)_{13}(MgO)_{87}$, were also prepared. The compositions were chosen to have a similar amount of Cu in different oxidation states. The mechanical treatment, reducing the crystallites to nanostructured dimensions, led to a high dispersion of the Cu–oxide phases in the MgO matrix. It can be noted that low and broadened peaks due to CuO are present in the $(CuO)_{13}(MgO)_{87}$ sample (Fig. 4, pattern a), and feeble signals due to $Cu_2O$ can be observed in the corresponding pattern relevant to $(Cu_2O)_7(MgO)_{93}$ (not shown). Even if a precise determination of the CuO and $Cu_2O$ coherent diffraction domains is complex because of their relatively small amounts in the mixtures, the estimated values in the range of 1.5–2.5 nm confirms the nanostructured features of the copper oxides (Table 2). As a consequence of the hydrogen pretreatment and chemical tests some metallic Cu was formed, as indicated by a shoulder in the main peak at $2\theta = 43.1$ and a small signal at $2\theta = 50.1$ (Fig. 4, patterns b and c). Even in these systems the JCPDS 30-794 MgO phase formed during the catalytic tests.

*XPS*

XPS measurements were performed *ex situ*; thus the surface of all samples were oxidized even after reduction (by $H_2$ or organic compounds). Carbonate contaminants were also developed due to air exposure.

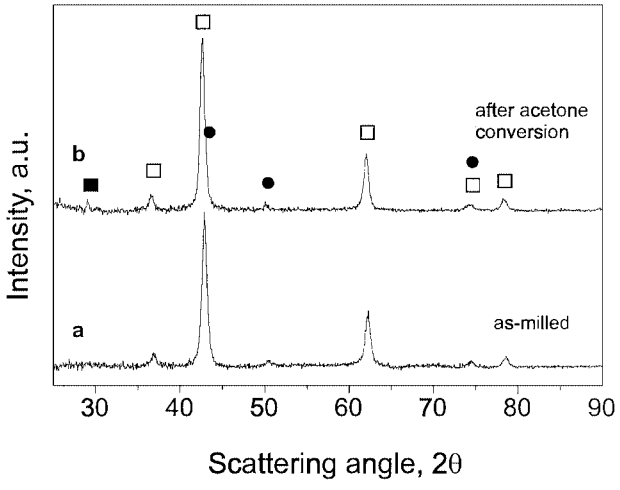


**FIG. 3.** XRD pattern of 3% Cu + MgO. (a) As-milled, (b) after reaction of acetone (6 h). ●, Cu (4–836); □, MgO (4–829); ■, MgO (30–794). Numbers of the corresponding JCPDS card files are given in parentheses.

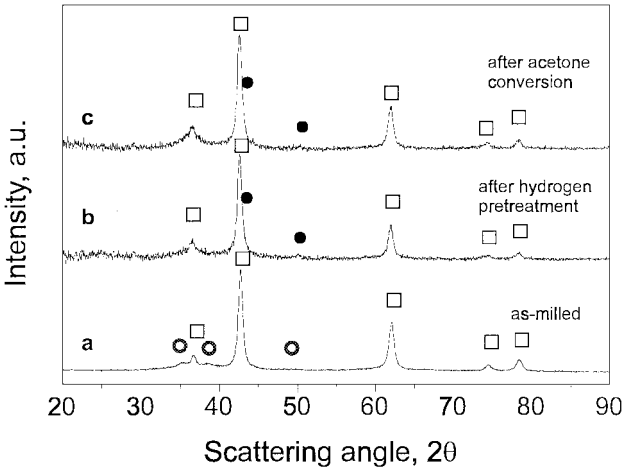


**FIG. 4.** XRD patterns of $(CuO)_{13}MgO_{87}$. (a) As-milled, (b) after hydrogen treatment (300°C, 1 h), (c) after reaction of acetone (1 h). ●, Cu (4–836); ○, CuO (41–254); □, MgO (4–829). Numbers of the corresponding JCPDS card files are given in parentheses.

The chemical compositions of the as-milled samples and the data of nominal bulk compositions are collected in Table 3 (this also includes data determined after reactions). The surface compositions usually differ from the nominal bulk ones, which can be attributed to the various mechanical and chemical treatments. It is seen that the actual surface concentrations of magnesium are always much lower than the nominal bulk values, and the same is true for copper for three of the five samples [$(Cu_2O)Mg(30)$, (CuO)Mg and 3% Cu + MgO]. Surface copper concentrations, in turn, exceed the nominal values for the $(Cu_2O)_7(MgO_{93})$ and $(CuO)_{13}(MgO_{87})$ mixed oxide samples. As a general phenomenon, substantial amounts of oxygen impurities are found on the surface [a significant amount of Na was also detected on $(Cu_2O)Mg(30)$]. On the other hand, the level of the carbon contamination of the as-milled samples and the residual carbon concentration after the reactions are relatively low. The composition changes during the pretreatment, and reactions are not significant, except for the $(Cu_2O)Mg(30)$ sample.

With respect to the surface chemical states of the main components, magnesium is oxidized; that is, it is in the $Mg^{2+}$ state in both oxide and carbonate environments. The carbon exists in hydrocarbon, carbonate, and to a small extent, carbide state. Copper is predominantly in the $Cu^{2+}$ state. The $Cu^0$ and $Cu^+$ forms could not be differentiated directly by the chemical shift of the Cu2p line. However, the intensity of the $2p_{3/2}$ main peak to its shake-up satellite, which is characteristic of the $Cu^{2+}$ chemical state, is 2.5 for the $(Cu_2O)_7(MgO)_{93}$ and 1.7 for the $(CuO)_{13}(MgO)_{87}$ mixed oxide samples (Fig. 5). The latter is the typical value for pure CuO samples (28).

**TABLE 3**

**Bulk and Surface Composition of the Cu–Mg–O Catalyst Systems (Atomic%) Determined by XPS**

| | | Cu | Mg | O | C[a] |
|---|---|---|---|---|---|
| $(Cu_2O)Mg(30)$ | Nominal in bulk | 50 | 25 | 25 | 0 |
| | As-milled[b] | 11.5 | 10.6 | 44.5 | 22.9 |
| | After reaction (2-propanol, 12 h)[b] | 17.0 | 6.7 | 44.5 | 15.9 |
| | After reaction (acetone, 6 h)[b] | 20.9 | 4.3 | 24.8 | 28.0 |
| (CuO)Mg | Nominal in bulk | 33.3 | 33.3 | 33.3 | 0 |
| | As-milled | 26.2 | 14.8 | 50.2 | 8.8 |
| 3% Cu + MgO | Nominal in bulk | 3 | 48.5 | 48.5 | 0 |
| | As-milled | 0 | 32.0 | 60.5 | 7.5 |
| | After reaction (acetone, 6 h) | 0.7 | 38.9 | 56.2 | 4.1 |
| $(Cu_2O)_7(MgO)_{93}$ | Nominal | 6.8 | 44.9 | 48.3 | 0 |
| | As-milled | 9.3 | 31.2 | 54.7 | 4.8 |
| | After reaction (acetone, 1 h) | 11.3 | 33.8 | 50.5 | 4.4 |
| $(CuO)_{13}(MgO)_{87}$ | Nominal in bulk | 6.5 | 43.5 | 50.0 | 0 |
| | As-milled | 9.5 | 28.7 | 54.8 | 7.0 |
| | After reaction (acetone, 1 h) | 7.2 | 35.9 | 52.5 | 4.5 |

[a] Sum of hydrocarbon, carbonate, and carbide chemical states.
[b] Na impurity was detected on the surface.

### *TPR and $Cu^0$ Measurements*

The results of temperature-programmed reduction of the samples are collected in Table 4 and shown in Figs. 6 and 7. Hydrogen consumption values determined with the as-milled samples without pretreatment should correspond to the quantity of ionic (reducible) copper present. Hydrogen consumption values for the two samples prepared by SSR [$(Cu_2O)Mg(30)$, (CuO)Mg] are very low compared to the

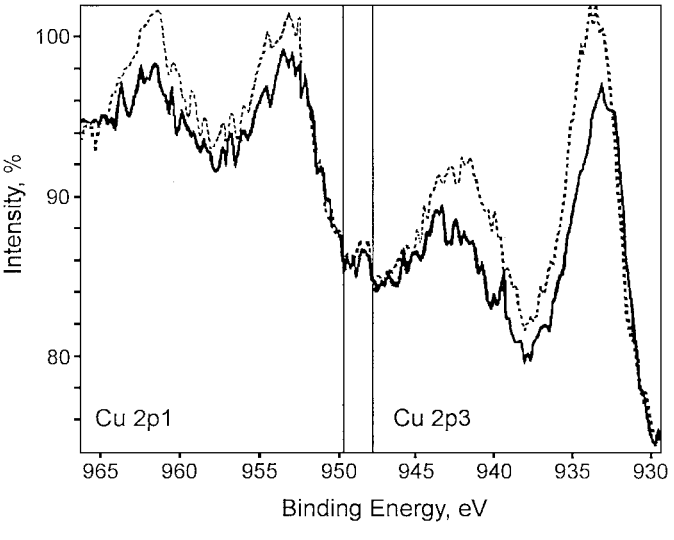


**FIG. 5.** Cu2p1 and Cu2p3 region of the XPS spectrum of the as-milled $(Cu_2O)_7(MgO)_{93}$ (solid line) and $(CuO)_{13}(MgO)_{87}$ (dotted line) samples.

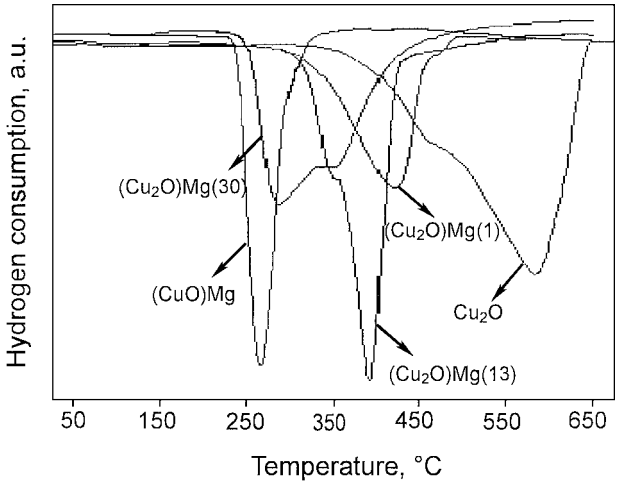


**FIG. 6.** TPR patterns of the $(Cu_2O)Mg$, $(CuO)Mg$, and $Cu_2O$ samples.

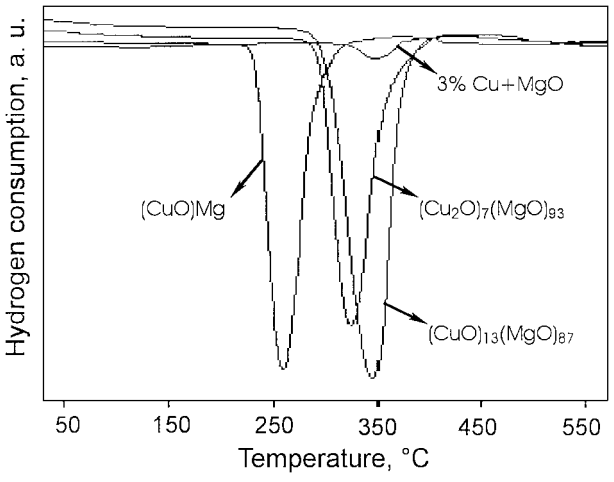


**FIG. 7.** TPR patterns of $(CuO)Mg$, 3% Cu + MgO, $(Cu_2O)_7(MgO)_{93}$, and $(CuO)_{13}(MgO)_{87}$.

theoretical values (Table 4, columns 2 and 3). The quantity of ionic copper, correspondingly, is also very low (Table 4, column 5). This conclusion is in agreement with XRD data indicating the almost complete transformation of copper oxides. Similar low values (low hydrogen consumption and low ionic copper content) were found for the 3% Cu + MgO sample. One should expect much higher values, however, when TPR is carried out following an oxidative pretreatment. Indeed, the values determined after oxidation of the samples (Table 4, column 4) are higher. These new values also indicate, however, that, at best, only rather small fractions of all Cu are accessible for reduction and oxidation in the as-milled state (Table 4, column 6).

In contrast, the reduction pattern of the remaining two samples [$(Cu_2O)_7(MgO)_{93}$, $(CuO)_{13}(MgO)_{87}$] is substantially different from those discussed previously. It is clear from a comparison of the two sets of data that, in these cases, most copper may be reduced and no substantial changes are brought about by oxidation. This is detected by XRD: CuO disappears and metallic copper appears in samples upon treatment with hydrogen (Fig. 4, pattern b). It also follows that copper is well-dispersed and in the +2 oxidation state. This latter conclusion is quite surprising for the $(Cu_2O)_7(MgO)_{93}$ sample. However, it is further supported by XPS data indicating that copper predominantly exists as $Cu^{2+}$ and the actual TPR profiles of the two specimens. In addition, for these two samples almost the total amount of copper present is reducible (Table 4, columns 5 and 6). $(Cu_2O)_{13}(MgO)_{87}$, however, shows a quite exceptional

**TABLE 4**

**Characterization of Samples by Chemical Methods**

| | Hydrogen consumed (mmol $g^{-1}$) | | | Cu composition[a] (%) | | |
|---|---|---|---|---|---|---|
| | Theoretical[b] | As-milled[c] | After oxidation[c] | Ionic Cu[d] | Total Cu[e] | $Cu^0$ on surface[f] |
| 1 | 2 | 3 | 4 | 5 | 6 | 7 |
| $(Cu_2O)Mg(1)$ | 11.9 | 0.72 | n.d.[g] | 6 | n.d. | n.d. |
| $(Cu_2O)Mg(13)$ | 11.9 | 1.07 | n.d. | 9 | n.d. | 0.2 |
| $(Cu_2O)Mg(30)$ | 11.9 | 1.07 | 1.76 | 9 | 15 | 0.3 |
| $(CuO)Mg$ | 9.6 | 1.85 | 3.22 | 19 | 34 | 2.5 |
| 3% Cu + MgO | 0.72 | 0.09 | 0.28 | 13 | 39 | 4.8 |
| $(Cu_2O)_7(MgO)_{93}$ | 2.29 | 1.70 | 2.07 | 74 | 90 | 14 |
| $(CuO)_{13}(MgO)_{87}$ | 2.29 | 2.41 | 2.01 | 100 | 88 | 17 |

[a] Values are relative to total nominal Cu as given in Table 1.
[b] Theoretical value of hydrogen consumption taking into account the quantity of Cu used in sample preparation, presumed to be present as CuO.
[c] Calculated using the quantity of hydrogen consumed during the TPR of CuO.
[d] Calculated from hydrogen consumption values of the as-milled state.
[e] Calculated from hydrogen consumption values measured after oxidation.
[f] Calculated from $N_2O$ decomposition data.
[g] Not determined.

behavior. Here all copper present may be reduced, but reducible copper decreases after oxidative treatment. This latter phenomenon may be attributed to sintering which is brought about by oxidation before TPR.

A comparison of the TPR profiles (Figs. 6 and 7) indicates that the samples studied have two copper species. (CuO)Mg shows a single reduction peak at 260°C, whereas the reduction temperature of the peak detected in 3% Cu + MgO, $(Cu_2O)_7(MgO)_{93}$, and $(CuO)_{13}(MgO)_{87}$ is about 350°C. The $(Cu_2O)$Mg(30) sample, in contrast, has a two-step reduction pattern with a peak maximum at about 270°C and a shoulder appearing at approximately 350°C, indicating that this sample has a mixture of the two copper species found in the other samples.

Previous studies with various supported copper catalysts established that bulk, crystalline CuO particles are reduced in the temperature range 200–260°C, whereas peak temperatures exceeding these values indicate the presence of copper species strongly interacting with the support (29–34). Among our samples, correspondingly, only (CuO)Mg [and, in part, $(Cu_2O)$Mg(30)] contains the easily reducible CuO phase, whereas the relatively high reduction temperature found for 3% Cu + MgO, $(Cu_2O)_7(MgO)_{93}$, and $(CuO)_{13}(MgO)_{87}$ testifies to the presence of the other species.

An analysis of the TPR profiles of the three $(Cu_2O)$Mg samples shows an interesting and important trend (Fig. 6). It is seen that the sample formed by the self-sustaining reaction undergoes reduction at a substantially lower temperature than does pure $Cu_2O$. Moreover, additional milling following the self-sustaining reaction further shifts peak maxima toward lower temperatures. As already shown in the literature (29, 30, 35) this may be attributed to increasing dispersion of copper, even though the actual dispersion values are rather low. Indeed, hydrogen consumption data (Table 4, columns 3 and 4), particle size values estimated from the XRD patterns (Table 2), and $Cu^0$ data determined by $N_2O$ decomposition (Table 2) are in agreement with this conclusion, that is, the quantity of surface copper increases (particle size values decrease) with increasing milling time. The change is particularly significant for the (CuO)Mg sample.

Interesting conclusions can be arrived at by comparing various data determined for copper found in the metallic state. The difference between the two sets of TPR data (Table 4, columns 5 and 6) give information about the relative quantity of metallic copper in the as-milled state. When these values are compared to those given in column 7, one can conclude that, in most cases, only a rather small fraction of metallic copper can be found on the surface.

Results of $Cu^0$ surface area measurements are also collected in Table 2 (last column). As the data show, $Cu^0$ values of three of the samples [(CuO)Mg, $(Cu_2O)_7(MgO_{93})$, and $(CuO)_{13}(MgO_{87})$] are about one order of magnitude higher than those of the other two specimens. Even these comparatively high values, however, correspond to rather low copper dispersions. It is also seen that, in most cases, particle sizes increase and, correspondingly, $Cu^0$ surface areas decrease during reaction.

### *Basicity Measurements*

2-Methyl-3-butyn-2-ol a well-studied probe molecule was chosen to test the basicity of the catalysts. The cleavage of this molecule to yield acetone and acetylene was suggested to correlate with basicity (26). In addition, acid sites were shown to catalyze dehydration to 3-methyl-3-buten-1-yne and skeletal isomerization to 3-methyl-2-butenal, whereas the formation of additional products (3-hydroxy-3-methyl-2-butanone and 3-methyl-3-buten-2-one) was attributed to the presence of acid–base pairs (26, 36). As pointed out in a recent comparative study, the possibility for these multipath transformations makes 2-methyl-3-butyn-2-ol a specific and especially useful probe molecule (37).

According to the data collected in Table 5 three samples prepared by starting mechanochemical treatment with MgO [the two mixed oxides $(Cu_2O)_7(MgO)_{93}$ and $(CuO)_{13}(MgO)_{87}$, and 3% Cu + MgO] exhibit the highest basicity, and basicity values parallel the MgO content of the samples. This is, naturally, not surprising. What is unexpected, however, is that the other two powders prepared by the self-sustaining reaction exhibit somewhat lower basicity. This is especially true for $(Cu_2O)$Mg(30), which required different experimental conditions (higher sample size and lower pulse size) to obtain accurate basicity values. It is also seen that basicity increases with increasing milling time. This seems to indicate that MgO formed as a result of a self-sustaining reaction may have a very low surface area. Prolonged milling, however, increases surface area; that is, more and more MgO is getting exposed to the surface.

**TABLE 5**

**Basicity of Samples Determined by Decomposition of 2-Methyl-3-butyn-2-ol and Condensation of Acetone**

| | 2-Methyl-3-butyn-2-ol[a] | | |
|---|---|---|---|
| | A[c] | B[d] | Acetone[b] |
| $(Cu_2O)$Mg(1) | 4 | — | — |
| $(Cu_2O)$Mg(13) | 11 | — | — |
| $(Cu_2O)$Mg(30) | 16 | 2 | 0 |
| (CuO)Mg | 61 | 20 | 6.8 |
| 3% Cu + MgO | — | 67 | 15.1 |
| $(Cu_2O)_7(MgO_{93})$ | — | 32 | 6.3 |
| $(CuO)_{13}(MgO_{87})$ | — | 31 | 5.9 |

[a] Conversion of 2-methyl-3-butyn-2-ol to acetylene and acetone (%).
[b] Conversion of acetone to mesityl oxide (%) after 1.5 h-on-stream.
[c] 50-mg sample size, 1-$\mu$l pulses.
[d] 10-mg sample size, 4-$\mu$l pulses.

Furthermore, the transformation of acetone was also studied without hydrogen in a flow system. We argued that this measurement should give an even more accurate estimate of the ability of the samples to induce dimerization, since it directly measures the reaction of acetone itself the starting material in the synthesis of MIBK. Data acquired in this way show the same tendency observed for 2-methyl-3-butyn-2-ol: 3% Cu + MgO exhibits the highest basicity, whereas the basicities of three other samples [(CuO)Mg, $(Cu_2O)_7(MgO)_{93}$, and $(CuO)_{13}(MgO)_{87}$] are practically the same. Again, $(Cu_2O)$Mg(30) proved to be the least basic material.

*Catalytic Studies*

The dehydrogenation of 2-propanol was studied with each powder sample to acquire information about the hydrogenating/dehydrogenating ability of the catalysts. In each case steady and high activity (better than 90% conversion) was observed. Illustrative of this is the activity pattern of four selected catalysts (Fig. 8.) $(Cu_2O)_7(MgO)_{93}$, the fifth sample, showed very similar activity to that of $(CuO)_{13}(MgO)_{87}$, the other mixed oxide, but these data were omitted for clarity. Dehydrogenation of 2-propanol yields acetone as the major product, but the formation of MIBK as the major by-product was always observed (Fig. 9). This indicates that the samples studied have a high ability to form MIBK: acetone, the product of dehydrogenation, immediately undergoes further transformations to produce MIBK even under the conditions of dehydrogenation.

The powder samples exhibited varying activities and selectivities in the synthesis of MIBK. Of the samples prepared by the SSR method, the catalytic activity of (CuO)Mg is significantly better than that of $(Cu_2O)$Mg(30) (Fig. 10),

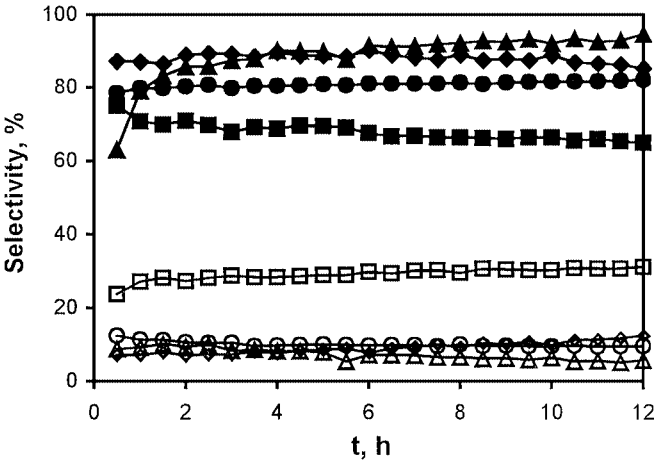


**FIG. 9.** Selectivity in the transformation of 2-propanol. ▲, △; $(Cu_2O)$Mg(30); ■, □, (CuO)Mg; ●, ○, 3% Cu + MgO; ◆, ◇, $(Cu_2O)_7(MgO)_{93}$. Closed symbols, selectivity of acetone; open symbols, selectivity of methyl isobutyl ketone. For reaction conditions, see Fig. 8.

whereas selectivities are practically identical (*vide infra*). For these measurements the optimal reaction conditions found in our earlier study for catalysts prepared by traditional methods were used (19). The catalytic performance of the mixed oxide samples, in turn, was unsatisfactory: although selectivities are rather high (60–90%), activities decreased steadily and rapidly during 6-h runs (Fig. 10).

The behavior of 3% Cu + MgO is rather interesting. Under the reaction conditions applied for the other four samples, this catalyst exhibited decreasing activity and rapidly decaying MIBK selectivity (Fig 11, squares). An analysis of product composition indicated, however, that the main product is mesityl oxide (Table 6), which is the intermediate formed in the second step of acetone transformation. It is clear, therefore, that mesityl oxide does not undergo the

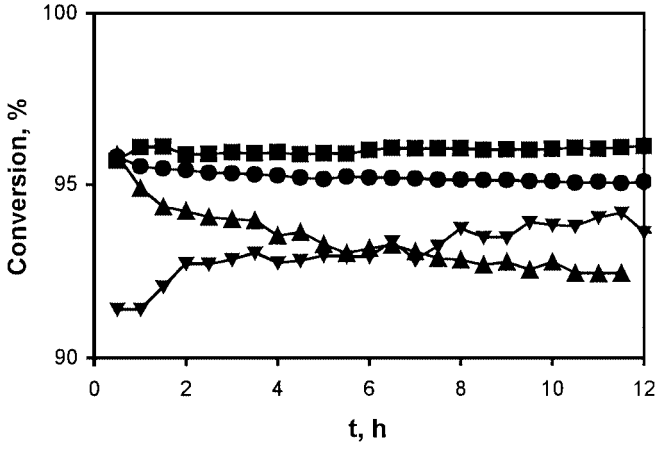


**FIG. 8.** The activity of catalysts in the transformation of 2-propanol. ▲, $(Cu_2O)$Mg(30); ■, (CuO)Mg; ●, 3% Cu + MgO; ▼, $(CuO)_{13}(MgO)_{87}$. Reaction conditions: temperature = 300°C, flow rate = 10 ml $min^{-1}$, 2-propanol to hydrogen molar ratio = 0.03.

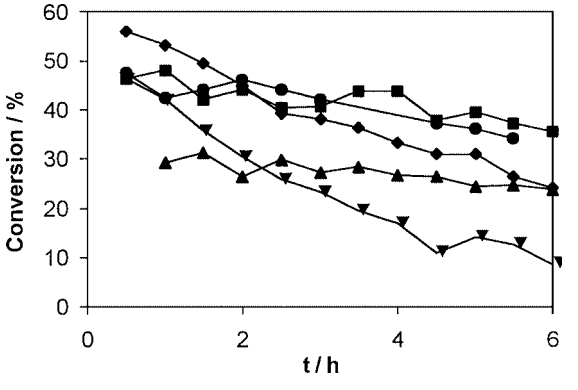


**FIG. 10.** Conversions in the transformation of acetone over $(Cu_2O)$Mg(30) (▲), (CuO)Mg (■), 3% Cu + MgO (●), $(Cu_2O)_7(MgO)_{93}$ and $(CuO)_{13}(MgO)_{87}$ (▼) powders. Reaction conditions, temperature = 280°C; flow rate = 8 ml $min^{-1}$; acetone-to-hydrogen molar ratio = 0.55, hydrogen/helium = 25 : 75. For reaction conditions for 3% Cu + MgO, see Fig. 8.

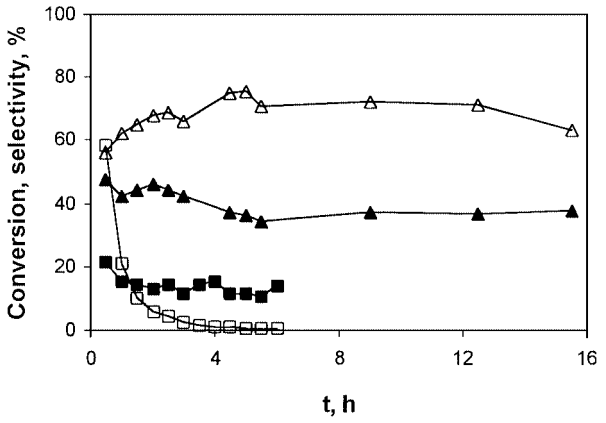


**FIG. 11.** Conversions and selectivities in the transformation of acetone over 3% Cu + MgO. Reaction conditions: for squares see Fig. 10; for triangles, see Fig. 8. ■, ▲, Conversion of acetone; □, △, selectivity of MIBK.

necessary hydrogenation to yield the end product MIBK under these reaction conditions. However, when the quantity of acetone and the acetone-to-hydrogen ratio were decreased, i.e., the hydrogen partial pressure was increased, satisfactory activity and selectivity could be attained (Fig 11, triangles). Unfortunately, these changes resulted in an increase in the undesired hydrogenation of acetone to 2-propanol (Table 6).

The results of the catalytic studies for the transformation of acetone to MIBK are collected for all samples in Table 7. It is rather difficult to give a comprehensive interpretation for all observations found and present a coherent picture. The samples, however, can be divided into two groups depending on their performance with respect to activities and selectivities.

The most important feature of samples made by a self-sustaining reaction [$(Cu_2O)Mg(30)$, (CuO)Mg] is their low MIBK selectivity. The reason for this appears to be their high activity to hydrogenate the carbon–oxygen double bond: the major side reaction over the SSR samples is overhydrogenation to produce MIBC. As discussed earlier, the main reduction peaks for these two samples are found at around 260–270°C (Figs. 6 and 7) which indicates that they have similar active copper species.

**TABLE 6**

**Effect of Temperature and Hydrogen Content on Conversion and Selectivity in the Synthesis of MIBK over 3% Cu + MgO[a]**

| Temperature (°C) | 280 | 300 |
|---|---|---|
| Acetone/hydrogen molar ratio | 0.55 | 0.03 |
| Conversion (%) | 11 | 36 |
| Selectivity | | |
| MIBK | 2 | 66 |
| MO | 95 | 3 |
| MIBC[b] | 0 | 5 |
| 2-Propanol | 0 | 19 |
| C9[c] | 3 | 7 |

[a] Values were determined at 3 h on stream.
[b] Methyl isobutyl carbinol (4-methyl-2-pentanol).
[c] Diisobutyl ketone and cyclic trimers.

**TABLE 7**

**Characteristic Data for the Synthesis of MIBK (Reaction Conditions: Temperature = 280°C, Flow Rate = 8 ml min$^{-1}$, Acetone-to-hydrogen Molar Ratio = 0.55, Hydrogen/Helium = 25 : 75)[a]**

| | | Selectivity (%) | | | | |
|---|---|---|---|---|---|---|
| | Conversion (%) | 2-Propanol | MIBK | MO | MIBC | C9 |
| $(Cu_2O)Mg(30)$ | 27 (27)[b] | 1 | 63 | 4 | 22 | 10 |
| (CuO)Mg | 41 (46) | 1.5 | 65 | 1.5 | 22 | 10 |
| 3% Cu + MgO | 36[c] (48) | 19 | 66 | 3 | 5 | 7 |
| $(Cu_2O)_7MgO_{93}$ | 38 (56) | 0.5 | 81 | 0.5 | 12 | 6 |
| | 6[d] | 1 | 90 | 1 | 5 | 3 |
| $(CuO)_{13}MgO_{87}$ | 23 (46) | 0 | 91 | 1 | 5 | 3 |
| | 10[d] | 0 | 62 | 38 | 0 | 0 |

[a] Data were determined at 3 h on stream.
[b] Initial activities measured at 0.5 h on stream are given in parentheses.
[c] Reaction conditions: temperature = 300°C, flow rate = 10 ml min$^{-1}$, acetone-to-hydrogen molar ratio = 0.03.
[d] Data were determined at 6 h on stream.

It is known that active site pairs composed of metallic copper and surface oxygen, or $Cu^0$ and ionic copper in close proximity, are required to hydrogenate the carbon–oxygen double bond (38, 39). According to TPR data, the SSR method, that is the *chemical transformation* between copper oxides and magnesium, specifically, the oxygen transfer from the oxides to magnesium, appears to produce active sites easily accommodating the surface oxygen needed for the hydrogenation of the ketone function. The low amount of 2-propanol formed over these two samples, however, is in apparent contradiction to this conclusion. This may be explained if we propose slow product desorption. Data in Table 4 (columns 5 and 6) show that the major part of copper of the two SSR samples is not available for either reduction or oxidation. One may surmise that these species, which may be tightly bound to the support can serve as strongly adsorbing sites hindering the desorption of MIBK thereby contributing to overhydrogenation.

Representatives of the other group are the two mixed oxides exhibiting very high MIBK selectivities. This is, obviously, due to their ability to hydrogenate the carbon–carbon double bond of MO to form the desired end product. This feature may be connected to their almost identical TPR profiles (Fig. 7) and the high initial $Cu^0$ surface areas (Table 2, last column).

The 3% Cu + MgO sample appears to be a unique case. On the basis of the identical preparation process and the high similarity of its TPR pattern to those of the mixed oxides (Fig. 7) similar characteristics in their catalytic

properties should be expected. In contrast, it shows a very low activity, completely different from that found for the mixed oxides, in the hydrogenation of MO under the usual reaction conditions (Table 6). Working under different reaction conditions, that is, applying high hydrogen partial pressure, greatly improves selectivity but with a cost: 2-propanol formed as a result of the hydrogenation of the starting material emerges as a new by-product. The very low copper content of this sample manifested by fast deactivation (Fig. 11) in combination with a possible support effect may contribute to the overall selectivity pattern of this sample. Further studies, however, are certainly needed to clarify this point.

It is somewhat surprising that the activity of the catalyst samples is rather similar despite the substantial differences measured for their basicity. Differences, however, do exist when initial activities are compared (Table 7): the least basic $(Cu_2O)Mg(30)$ sample shows the lowest activity. In addition, the two SSR samples with low basicity exhibit rather stable activities. In all other cases activities decrease substantially during time on stream. Basic sites are able to promote various types of condensation reactions leading to high-molecular-weight by-products not detected in the liquid reaction products. The accumulation of such products on the strongest basic sites and the increase in MgO particle size (Table 2) are the possible reasons for decreasing and similar activities. The decrease in activity is especially marked in the case of the mixed oxides. Here, a combination of two factors, poisoning of basic sites and the rapid aggregation of the metal particles under reaction conditions as indicated by TPR and $Cu^0$ data, may account for the observed phenomenon.

## CONCLUSIONS

High-energy ball milling was found to be a suitable method to prepare Cu–MgO catalyst systems for application in the one-step synthesis of MIBK. The nanocrystalline powders thus prepared have ionic (reducible) and metallic copper species in widely varying amounts. The samples produced by SSR exhibit a high ability to hydrogenate the carbon–oxygen double bond resulting in low MIBK selectivity. The mixed oxides, in turn, are more active in the hydrogenation of the carbon–carbon double bond of MO thereby exhibiting high MIBK selectivity. These features may be accounted for by the relative population of two different copper species detected by TPR, namely, bulk CuO with low reduction temperature (260°C) and species strongly interacting with the support with a reduction temperature of about 350°C.

## ACKNOWLEDGMENTS

The XPS characterization was performed in the ESCA Laboratory of the OTKA Materials Science Measuring Center (Budapest). Financial support for this work by the National Research Foundation of Hungary (Grant OTKA T030156) is highly appreciated.

## REFERENCES

1. N. Z. Lyakhov, Ed., "Chemistry of Sustainable Development," Vol. 6. Proceedings, INCOME-2, 1998, Siberian Branch of the Russian Academy of Sciences, Novosibirsk.
2. J. Eckert, H. Schlorb, and L. Schultz, Eds., *J. Metastable Nanocryst. Mater*. **8**, Proceedings, ISMANAM-99, 2000, Trans Tech Publications, Zurich.
3. Merzhanov, A. G., *Int. J. Self Propagating High Temp. Synth*. **4**, 323 (1995).
4. Takacs, L., *Mater. Sci. Forum* **269–272**, 513 (1998).
5. Cocco, G., Mulas, G., and Schiffini, L., *Mater. Sci. Forum* **179–181**, 281 (1995).
6. Brower, W. E., Montes, A. J., Prudlov, K. A., Bakker, H., and Moleman, A. C., Yang, H., *Mater. Sci. Forum* **235–238**, 935 (1997).
7. Zhang, H. F., Li, J., Song, Q. H., and Hu, Z. Q., *J. Mater. Res*. **13**, 281 (1995).
8. Mulas, G., Deledda, S., Monagheddu, M., Cocco, G., Cutrufello, M. G., Ferino, I., and Solinas, V., *J. Metastable Nanocryst. Mater*. **8**, 889 (2000).
9. Mulas, G., Varga, M., Bertóti, I., Molnár, Á., Cocco, G., and Szépvölgyi, J., *Mater. Sci. Eng., A* **267**, 193 (1999).
10. Molnár, Á., Varga, M., Mulas, G., Mohai, M., Bertóti, I., Lovas, A., and Cocco, G., *Mater. Sci. Eng., A* **304–306**, 1078 (2001).
11. Braithwaite, J., *in* "Kirk-Othmer Encyclopedia of Chemical Technology" (J. I. Kroschwitz and M. Howe-Grant, Eds.), 4th edition, Vol. 14, p. 989. Wiley, New York, 1995.
12. Unnikrishnan, R., and Narayanan, S., *J. Mol. Catal. A Chem*. **144**, 173 (1999).
13. Melo, L., Giannetto, G., Alvarez, F., Magnoux, P., and Guisnet, M., *Catal. Lett*. **44**, 201 (1997).
14. Lin, K.-H., and Ko, A.-N., *Appl. Catal. A* **147**, L259 (1996).
15. Chen, Y. Z., Liaw, B. J., Tan, H. R., and Shen, K. L., *Appl. Catal. A* **205**, 61 (2001).
16. Higashio, Y., and Nakayama, T., *Catal. Today* **28**, 127 (1996).
17. Nikolopoluos, A. A., Howe, G. B., Jang, W.-L., Subramanian, R., Spivey, J. J., Olsen, D. J., Devon, T. J., and Culp, R. D. , *in* "Catalysis of Organic Reactions" (M. E. Ford, Ed.), p. 533. Dekker, New York, 2000.
18. Das, N., Tichit, D., Durand, R., Graffin, P., and Coq, B., *Catal. Lett*. **71**, 181 (2001).
19. Chikán, V., Molnár, Á., and Balázsik, K., *J. Catal*. **184**, 134 (1999).
20. Rietveld, H. M., *J. Appl. Crystallogr.* **2**, 65 (1969).
21. Lutterotti, L., Ceccato, R., Dal Maschio, R., and Pagani, E., *Mater. Sci. Forum* **278–281**, 87 (1998).
22. Mohai, M., *Surf. Interface Anal*., to be published.
23. Mohai, M., and Bertóti, I., "ECASIA 95" (H. J. Mathieu, B. Reihl, and D. Briggs, Eds.), p. 675. Wiley, Chichester, 1995.
24. Evans, S., Pritchard, R. G., and Thomas, J. M., *J. Electron Spectrosc. Relat. Phenom*. **14**, 341 (1978).
25. Reilman, R. F., Msezane, A., and Manson, S. T., *J. Electron Spectrosc. Relat. Phenom*. **8**, 389 (1976).
26. Lauron-Pernot, H., Luck, F., and Popa, J. M., *Appl. Catal*. **78**, 213 (1991).
27. Mulas, G., Deledda, S., and Cocco, G., *Mater. Sci. Eng., A* **267**, 214 (1999).
28. Tobin, J. P., Hischwald, W., and Cunningham, J., *Appl. Surf. Sci*. **16**, 441 (1983).
29. Dow, W.-P., Wang, Y.-P., and Huang, T.-J., *J. Catal*. **160**, 155 (1996).

30. Gredig, S. V., Maurere, R., Koeppel, R. A., and Baiker, A., *J. Mol. Catal. A Chem*. **127**, 133 (1997).
31. Boccuzzi, F., Chiorino, A., Martra, G., Gargano, M., Ravasio, N., and Carrozzini, B., *J. Catal*. **165**, 129 (1997).
32. Anderson, J. A., Márquez-Alvarez, C., López-Munoz, M. J., Rodrígez-Ramos, I., and Guerrero-Ruiz, A., *Appl. Catal. B* **14**, 189 (1997).
33. Carniti, P., Gervasini, A., Modica, V. H., and Ravasio, N., *Appl. Catal. B* **28**, 175 (2000).
34. Suh, Y.-W., Moon, S.-H., and Rhee, H.-K., *Catal. Today* **63**, 447 (2000).
35. Galvagno, S., Crisafulli, C., Maggiore, R., Touszik, G. R., and Giannnetto, A., *J. Therm. Anal.* **30**, 611 (1985).
36. Huang, M., and Kaliaguine, S., *Catal. Lett*. **18**, 373 (1993).
37. Aramendía, M. A., Boráu, V., García, I. M., Jiménez, C., Marinas, A., Marinas, J. M., Porras, A., and Urbano, F. J., *Appl. Catal. A* **184**, 115 (1999).
38. Cunningham, J., Al-Sayyed, G. H., Cronin, J. A., Healy, C., and Hirschwald, W., *Appl. Catal*. **25**, 129 (1986).
39. Cunningham, J., McNamara, D., Fierro, J. L. G., and O'Brian, S., *Appl. Catal*. **35**, 381 (1987).